

# Extensive but Coordinated Reorganization of the Membrane Skeleton in Myofibers of Dystrophic (*mdx*) Mice

McRae W. Williams and Robert J. Bloch

Department of Physiology, School of Medicine, University of Maryland, Baltimore, Maryland 21201

**Abstract.** We used immunofluorescence techniques and confocal imaging to study the organization of the membrane skeleton of skeletal muscle fibers of *mdx* mice, which lack dystrophin.  $\beta$ -Spectrin is normally found at the sarcolemma in costameres, a rectilinear array of longitudinal strands and elements overlying Z and M lines. However, in the skeletal muscle of *mdx* mice,  $\beta$ -spectrin tends to be absent from the sarcolemma over M lines and the longitudinal strands may be disrupted or missing. Other proteins of the membrane and associated cytoskeleton, including syntrophin,  $\beta$ -dystroglycan, vinculin, and Na,K-ATPase are also concentrated in costameres, in control myofibers, and *mdx* muscle. They also distribute into the same altered sarcolemmal arrays that contain  $\beta$ -spectrin. Utro-

phin, which is expressed in *mdx* muscle, also codistributes with  $\beta$ -spectrin at the mutant sarcolemma. By contrast, the distribution of structural and intracellular membrane proteins, including  $\alpha$ -actinin, the Ca-ATPase and dihydropyridine receptors, is not affected, even at sites close to the sarcolemma. Our results suggest that in myofibers of the *mdx* mouse, the membrane-associated cytoskeleton, but not the nearby myoplasm, undergoes widespread coordinated changes in organization. These changes may contribute to the fragility of the sarcolemma of dystrophic muscle.

**Key words:** sarcolemma • membrane skeleton • muscular dystrophy • spectrin • dystrophin

**D**YSTROPHIN is the protein that is missing or mutated in patients with Duchenne or Becker muscular dystrophy (for review see 22, 23) and in the *mdx* mouse (6, 80). The absence of dystrophin is believed to weaken the sarcolemma, which becomes more susceptible to damage during the contractile cycle (22, 52, 74). How dystrophin stabilizes the sarcolemma of healthy muscle fibers and how its loss destabilizes the sarcolemma of dystrophic fibers are still poorly understood, despite the extensive molecular characterization of dystrophin and its ligands.

Molecular cloning and sequencing of dystrophin place it in the spectrin superfamily of cytoskeletal proteins (1, 15, 17, 40, 43). Like other members of this superfamily, including  $\alpha$ -actinin and  $\beta$ -spectrin, dystrophin has an NH<sub>2</sub>-terminal domain that binds actin and a central rod domain composed of a series of triple helical repeats. Like  $\alpha$ -actinin and  $\alpha$ -spectrin, dystrophin has a sequence in its COOH-terminal region containing EF hands. The COOH-terminal domain of dystrophin also binds a complex of integral membrane glycoproteins that includes dystroglycan and

the sarcoglycans (8, 35, 57, 85). Analysis of the severity of the myopathies caused by different mutations of dystrophin in humans and in transgenic *mdx* mice suggests that changes limited to the central rod domain and the actin-binding domain have relatively modest effects. However, changes that inhibit binding to the glycoprotein complex are associated with the severest forms of dystrophy (10, 24, 65, 84).

Some of these changes associated with binding to the glycoprotein complex are likely to be related to extracellular structures, as dystroglycan (also known as cranin) binds laminin with high affinity (26, 35, 70). Thus, the dystrophin-glycoprotein complex has the potential of linking actin in the sarcomeres of superficial myofibrils through dystrophin and the trans-sarcolemmal glycoprotein complex, to laminin in the basal lamina of the muscle fiber. This role of the dystrophin-glycoprotein complex is consistent with the observation that dystrophin is concentrated at the sarcolemma of skeletal muscle fibers in costameres, regions of the sarcolemma that overlie Z and M lines, as well as in longitudinally oriented strands (47, 49, 62, 73). Costameres are believed to be involved in linking the contractile apparatus to the basal lamina (60, 69, 75). Thus, they may serve to transmit the force of contraction to extracellular elements (75). Mutations that alter this linkage would be expected to alter the stresses on the sarcolemma that occur

Address correspondence to Robert J. Bloch, 660 W. Redwood St., Baltimore, MD 21201. Tel. and Fax: (410) 706-8341. E-mail: rbloch@umaryland.edu

during contraction, perhaps resulting in tears in the membrane that lead to the formation of delta lesions (52). This force transmission model for the damage caused in muscular dystrophy is consistent with nearly all the current structural and genetic evidence with one notable exception: it does not account for the mild effects of mutations affecting dystrophin-actin binding.

As an alternative to this model for the physiological role of dystrophin, we are examining the possibility that the fragility of the sarcolemma in dystrophic myofibers is linked to changes in the organization of the membrane-associated cytoskeleton. Dystrophin is only one of several structural proteins that underlie and support the sarcolemma. We hypothesize that, in the absence of dystrophin, changes in the organization of these other structural proteins may leave the sarcolemma vulnerable to damage. This idea is based on earlier observations that  $\beta$ -spectrin and vinculin colocalize with dystrophin in the costameres of skeletal muscle fibers (62). Furthermore, our earlier results suggested that, although  $\beta$ -spectrin remained associated with the sarcolemma in human and mouse muscle fibers that lacked dystrophin, its distribution at the membrane was abnormal (62; see also 20, 50). Here we provide morphological evidence that the membrane skeletal proteins of dystrophic, *mdx* mice codistribute in abnormal sarcolemmal structures. These morphological changes leave extensive regions of the membrane with little apparent support from the membrane skeleton and may contribute to the fragility of the sarcolemma of dystrophic muscle.

## Materials and Methods

### Animals

All mice (Jackson Laboratories) used were male C57-black-10smcDMD-*mdx* mice and control littermates aged 6 mo.

### Tissue for Immunofluorescence

Animals were anesthetized by intraperitoneal injection of a combination of ketamine (80 mg/kg) and xylazine (7 mg/kg). Fixed tissue was obtained by perfusing the anesthetized animal through the left ventricle with a solution of 2% paraformaldehyde in PBS (10 mM NaP, 145 mM NaCl, pH 7.2). Fast twitch muscles, including the tibialis anterior, extensor digitorum longus, and quadriceps muscles, were dissected; the quadriceps muscle was incubated for an additional 5 min in 2% paraformaldehyde in PBS. Tissue was blotted dry and placed on a cryostat chuck in O.C.T. mounting medium (4583 tissue tek; Skura Finetek USA, Inc.). The chuck was plunged into a slush of liquid nitrogen, generated under vacuum. 20- $\mu$ m-thick sections were cut on a cryostat (model 2800, Frigocut, Reichart-Jung, Cambridge Instruments), collected on glass slides coated with 0.5% gelatin and 0.05% chromium potassium sulfate, and stored desiccated at  $-70^{\circ}\text{C}$ .

For the preparation of unfixed longitudinal sections, tissue was obtained without perfusion, mounted, frozen, and cryosectioned as above. To prevent contraction, the frozen sections were collected on the surface of an ice-cold bath of PBS containing 10 mM EGTA, pH 7.4. Sections were rapidly lifted from the surface of the bath directly onto gelatin-coated slides. Unfixed longitudinal sections were cut fresh for each experiment and used immediately.

### Antibodies

Mouse mAbs (Novocastra Laboratories) to the COOH terminus (amino acids 3669–3685) of human dystrophin (Dys2; ref. 54), to the COOH terminus of human  $\beta$ -dystroglycan (5), and to a fusion protein containing the NH<sub>2</sub>-terminal region of utrophin (NCL-DRP-2; ref. 4) were used at dilutions of 1:5, 1:10, and 1:5, respectively. An mAb against all known syntro-

phin isoforms, 1351, was provided by Dr. S. Froehner (University of North Carolina, Chapel Hill, NC), and was used at 16  $\mu\text{g/ml}$ . Mouse mAbs (Affinity Bioreagents) against the  $\alpha$  subunit of the dihydropyridine receptor (DHPR<sup>1</sup>; clone 1A), and the sarcoplasmic/endoplasmic reticulum Ca-ATPase from rabbit skeletal muscle (SERCA 1) were used at dilutions of 1:200 and 1:100, respectively. Mouse mAbs against  $\alpha$ -actinin from rabbit skeletal muscle (EA-53) and vinculin from chicken gizzard (VIN-11-5; both from Sigma Immuno Chemicals) were used at dilutions of 1:200 and 1:50, respectively.

The rabbit polyclonal antibody, 9050, was prepared against purified human erythrocyte  $\beta$ -spectrin. It was affinity-purified over a column of erythrocyte  $\beta$ -spectrin and cross-adsorbed against  $\beta$ -fodrin and  $\alpha$ -fodrin, purified from bovine brain as previously described (63, 87). Antibodies to erythrocyte  $\beta$ -spectrin were also generated in chickens. IgY was purified from egg yolk using the EggExtract kit (Promega Corp.) and anti- $\beta$ -spectrin antibodies were affinity-purified as described (63). Specificity for  $\beta$ -spectrin was demonstrated by immunoblotting (Ursitti, J.A., L. Martin, W.G. Resneck, T. Chaney, C. Zielke, B.E. Alger, and R.J. Bloch, manuscript submitted for publication). Both affinity-purified antibodies to  $\beta$ -spectrin were used at 3  $\mu\text{g/ml}$ . Polyclonal rabbit antibodies to a fusion protein containing residues 335–519 of the  $\alpha$ 1 subunit of the Na,K-ATPase and to a fusion protein containing residues 338–519 of the  $\alpha$ 2 subunit of the Na,K-ATPase (Upstate Biotechnologies) were used at 3  $\mu\text{g/ml}$ .

Nonimmune mouse mAbs, MOPC21, were obtained from Sigma Chemical Co. Nonimmune chicken IgY was purified from preimmune controls collected from the same chickens and used to generate the anti- $\beta$ -spectrin antibodies. Normal rabbit serum was purchased from Jackson ImmunoResearch Laboratories.

Secondary antibodies included goat anti-rabbit and goat anti-mouse IgGs, and donkey anti-chicken IgY. All secondary antibodies (Jackson ImmunoResearch) as fluorescein or tetramethylrhodamine conjugates were species-specific with minimal cross-reactivity and were used at a dilution of 1:100.

The specificities of all these antibodies have been established by immunoblotting or immunoprecipitation, as reported by the suppliers or in the relevant publications.

### Fluorescent Immunolabeling

Sections were incubated in PBS/BSA (PBS containing 1 mg/ml BSA and 10 mM NaN<sub>3</sub>) for 15 min to reduce nonspecific binding and placed in primary antibody in PBS/BSA for 2 h at room temperature, or overnight at 4°C. Samples were washed with PBS/BSA and incubated for 1 h with fluorescein- or tetramethylrhodamine-conjugated secondary antibodies diluted in PBS/BSA. After additional washing, samples were mounted in a solution containing nine parts glycerol, one part 1 M Tris-HCl, pH 8.0, supplemented with 1 mg/ml *p*-phenylenediamine to reduce photobleaching (37). Slides were observed with a Zeiss 410 confocal laser scanning microscope (Carl Zeiss, Inc.) equipped with a 63 $\times$  NA 1.4 plan-apochromatic objective. The pinholes for both fluorescein and tetramethylrhodamine fluorescence were set to 18. Images were collected and stored with software provided by Zeiss.

To generate figures, images were arranged into montages, labeled, and given scale bars with Corel Draw 6 (Corel Corporation Ltd.). Inset pictures were prepared with MetaMorph (Universal Imaging) and magnified twofold with Corel Draw 6. No other processing was used on any of the images.

For the quantitations shown in Fig. 3, images were prepared by one of the authors and scored double blind by the other. Images were taken of all sarcolemmal regions in controls and *mdx* myofibers that did not show obvious tears, holes, or other processing artifacts. Sampling was otherwise random. Images of control and *mdx* sarcolemma were coded and mixed randomly. Each image was then evaluated for the pattern of  $\beta$ -spectrin distribution that was most common over the region of the sarcolemma in clear focus. Images were sorted into one of four categories: clear costameric distribution, including regular labeling over Z and M lines and in longitudinal domains; label present at Z lines, but absent over M lines or in longitudinal domains; label present at Z lines but absent both over M lines and in longitudinal domains; and label absent at Z lines, M lines, and longitudinal domains, but present in polygonal arrays or other irregular structures. We obtained consistent results when other naive observers scored the same or a similar set of images.

1. *Abbreviations used in this paper:* DHPR, dihydropyridine receptor; SERCA, Ca-ATPase of the sarcoplasmic reticulum.

## Materials

Unless otherwise stated, all materials were purchased from Sigma Chemical Co. and were the highest grade available.

## Results

We used immunofluorescence labeling and confocal microscopy to examine the distribution of several membrane skeletal proteins in longitudinal sections through the sarcolemma of fast twitch muscle fibers from the dystrophic *mdx* mouse. The use of confocal optics allowed us to isolate the fluorescence signal arising from proteins located within  $\sim 1.2 \mu\text{m}$  of the sarcolemmal bilayer (83), thereby reducing any fluorescence signals, specific or nonspecific, associated with structures lying deeper in the myoplasm. Each of the sarcolemmal proteins we examined has been shown to be concentrated in costameres, together with dystrophin and  $\beta$ -spectrin (12, 32, 47, 49, 59, 62, 73; Williams, M.W., and R.J. Bloch, manuscript in preparation). We limited our observations to fast twitch fibers because the rectilinear pattern generated by immunolabeling of membrane skeletal elements at the sarcolemma, overlying Z and M lines and in longitudinally oriented strands, is much more clearly defined than in slow twitch fibers (Williams, M.W., and R.J. Bloch, manuscript in preparation). In addition, fast twitch fibers are more susceptible to damage associated with dystrophinopathies (82).

### $\beta$ -Spectrin in *mdx* Muscle

Longitudinal cryosections were prepared from the quadriceps muscle of control and *mdx* mice. Sections from control and *mdx* samples were placed on the same slides and were treated simultaneously during all stages of our experiments. We first labeled sections with 9050, an affinity-purified polyclonal antibody against  $\beta$ -spectrin, and Dys2, an mAb against dystrophin. Primary antibodies were visualized with species-specific secondary antibodies coupled to either fluorescein or tetramethylrhodamine. In controls,  $\beta$ -spectrin was found in costameres, areas overlying the Z lines and M lines, and in longitudinally oriented strands (Fig. 1 A, arrows and arrowheads indicate examples of each of these structures), as we reported previously (62; see also 12). In our samples, costameres overlying Z and M lines could be distinguished under fluorescence illumination by the fact that structures over Z lines were usually wider than those over M lines (62). Labeling of all these structures was specific, as it was not obtained in either wild-type (Fig. 1, G and H) or *mdx* tissue (Fig. 1, K and L) with nonimmune rabbit antibodies or with a secondary antibody that failed to bind rabbit IgG. Dystrophin, recognized by labeling with Dys2, was also enriched in costameres (Fig. 1 B), as previously reported (47, 49, 62, 73).

The distribution of  $\beta$ -spectrin in the quadriceps of the *mdx* mouse differed significantly from that in control muscles. Although in some cases the  $\beta$ -spectrin distribution was very similar to that seen in the control tissue (Fig. 2, normal rectilinear distribution) such examples were rare in *mdx* muscle ( $<3\%$  of 108 fibers scored double blind). Many of the samples ( $\sim 36\%$ ) failed to show labeling for

$\beta$ -spectrin either over M lines (Fig. 2, E and F) or in longitudinally oriented strands (Fig. 2, C and D). Approximately the same proportion of *mdx* fibers ( $\sim 42\%$ ) failed to show labeling of both these structures (Fig. 2, G and H), and so retained organized domains of  $\beta$ -spectrin only over Z lines. This pattern of labeling is similar to that reported by Porter et al. (62), Minetti et al. (50), and Ehmer et al. (20). The *mdx* muscle fibers that could not be placed into any of the above categories showed different morphologies, including small irregular boxes, zig-zag patterns, or polygonal arrays (Fig. 2, I–L). Some regions of the sarcolemma of *mdx* muscle lacking visible  $\beta$ -spectrin extended over several sarcomeres (Fig. 2 J, inset) or encompassed large areas ( $>50 \mu\text{m}^2$ ) of the sarcolemma between Z lines (Fig. 2 H). The fact that all of these patterns were associated with muscle fibers that lacked dystrophin was confirmed by double immunofluorescence studies with anti- $\beta$ -spectrin and Dys2 anti-dystrophin. The latter antibody did not label any structures at the sarcolemma of the dystrophic muscle fibers studied here (not shown).

In contrast to our results with *mdx* muscle fibers, we found that  $>75\%$  of control myofibers had regular rectilinear distributions of  $\beta$ -spectrin at the sarcolemma (Figs. 1 A and 2 A), with prominent elements in longitudinally oriented strands and overlying Z and M lines. Most of the remaining control fibers were not labeled at the sarcolemma either over M lines or in longitudinal domains. Only one control fiber out of the 72 that we scored did not show labeling of the sarcolemma over M lines or longitudinal domains. We found no control fibers with irregular boxes, polygonal arrays, or zig-zag patterns as seen in *mdx*. Typically, the regions of the control sarcolemma that failed to label with antibodies to  $\beta$ -spectrin extended over areas of only  $1\text{--}2 \mu\text{m}^2$  (the area enclosed by adjacent Z and M lines and a pair of well-spaced longitudinal strands) in control muscle fibers. In very few cases ( $<1\%$  of all fibers in controls and *mdx*), we found regions of the sarcolemma of muscle fibers that showed little or no organization of the sarcolemma. These may represent regions that were poorly preserved or damaged during processing.

The altered arrangement of proteins at the sarcolemma of dystrophic muscle fibers was not due to differences in fixation or labeling of these fibers. We routinely examined samples that were fixed by perfusion in situ before the muscle was dissected and cryosectioned, as well as samples that were unfixed and collected under conditions that prevented contraction following cryosectioning (see Materials and Methods). To examine their possible effects, we also varied the perfusion and fixation regimens. We found no significant differences among these samples, suggesting that our results were independent of the methods we used. Furthermore, control and *mdx* samples were matched for age and sex, so these factors did not contribute to the differences in sarcolemmal organization. Finally, most control and *mdx* samples were also collected, frozen, sectioned, and stained together. Therefore, this ruled out the possibility that differences in handling could account for the morphological changes we observed. These results suggest that the organization of  $\beta$ -spectrin at the sarcolemma of *mdx* is altered from the control. The differences between the *mdx* and control samples, summarized in Fig. 3, are highly significant ( $P < 0.0001$  by  $\chi^2$  analysis).

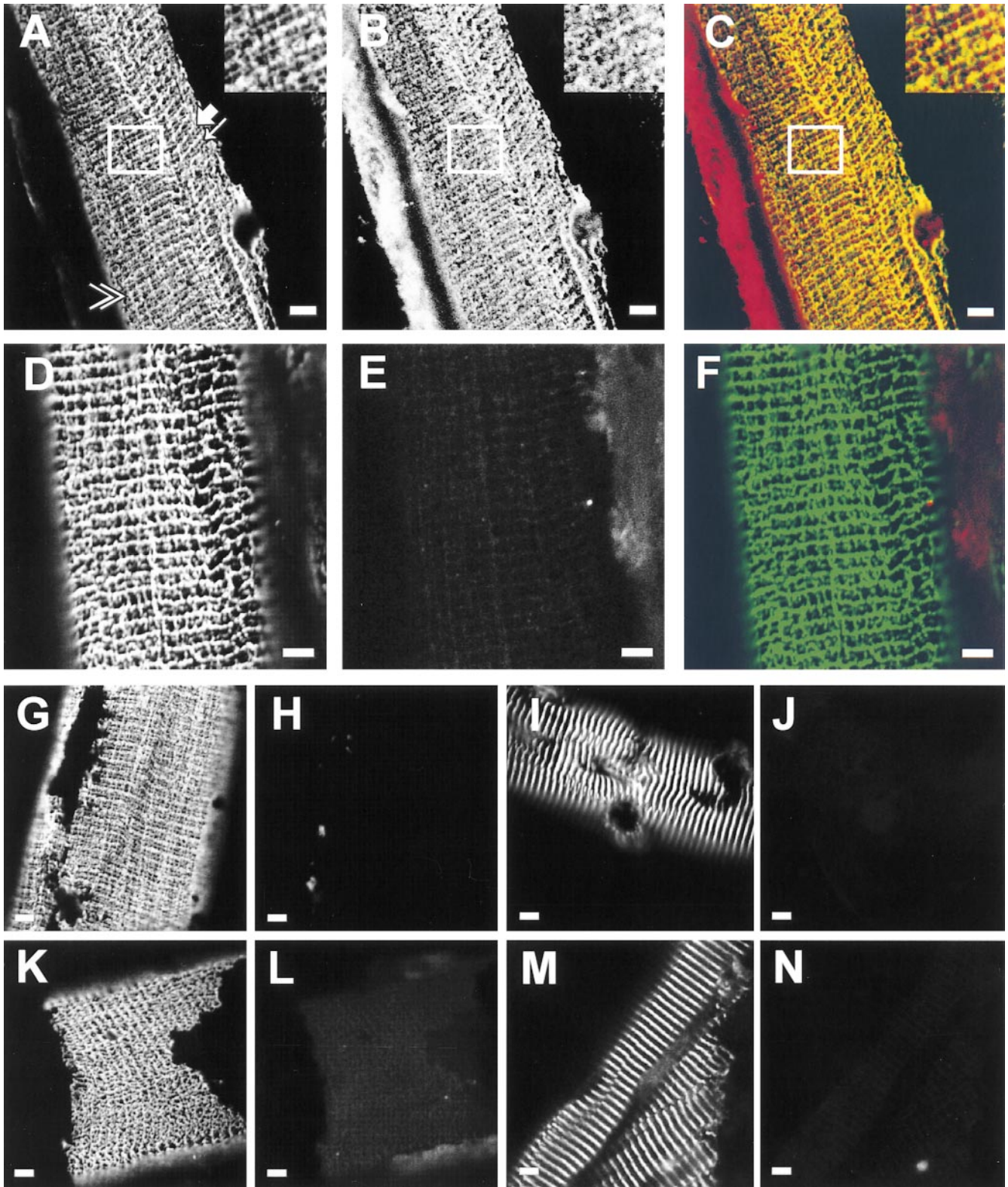


**Figure 1.** Immunolabeling of  $\beta$ -spectrin and dystrophin in wild-type and *mdx* muscle. Perfusion-fixed quadriceps muscles from wild-type (A–C, G–J) and *mdx* mice (D–F, K–N) were snap frozen, and cryosectioned (see Materials and Methods). The sections were double-labeled with affinity-purified rabbit antibodies (9050) to  $\beta$ -spectrin (A and D) and with the mouse mAb, Dys2, to dystrophin (B and E). Typical costameric structures overlying a Z line (thick arrow), an M line (thin arrow), and in a longitudinal strand (double arrowheads) are indicated in A. Color composite images were created to show  $\beta$ -spectrin in green, dystrophin in red, and areas containing both proteins in yellow (C and F). These images show extensive overlap of labeling for  $\beta$ -spectrin and dystrophin in costameres of wild-type (C) but not *mdx* (F) muscle. Controls were double-labeled with 9050 (G and K) and MOPC21, a nonimmune mouse mAb (H and L), or with a mouse mAb to  $\alpha$ -actinin (I and M) and normal rabbit serum (J and N). Control samples, imaged under conditions identical to those used in A–F, showed little nonspecific labeling or bleedthrough of fluorescence. This was also true for the *mdx* sample shown in D–F. Bars, 5  $\mu$ m.



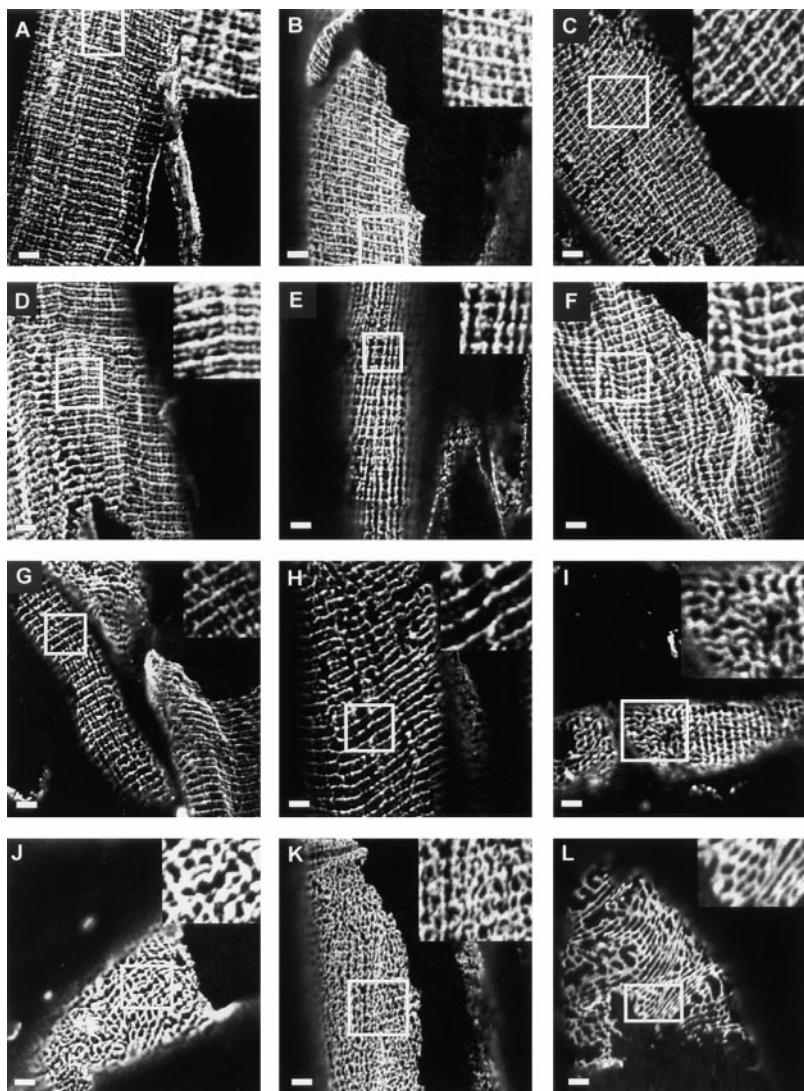


**Figure 2.** Altered distribution of  $\beta$ -spectrin at the sarcolemma of *mdx* muscle fibers. Samples were processed as in Fig. 1 and labeled with 9050 rabbit anti- $\beta$ -spectrin antibodies. Control fibers show a clear costameric distribution for  $\beta$ -spectrin (A). Fibers from the *mdx* mouse show a range of distributions of  $\beta$ -spectrin (B-L), from normal (B) to highly altered (J-L). In most *mdx* fibers,  $\beta$ -spectrin was depleted or missing at the sarcolemma in longitudinal domains (C and D), overlying M lines (E and F), or both (G and H). In some regions,  $\beta$ -spectrin could not be detected at the sarcolemma overlying some Z lines (I-L), which led to the formation of zig-zag patterns (I and J) or polygonal arrays (K and L). Bars, 5  $\mu$ m. Inserts show the regions enclosed by white boxes at twofold magnification.

### Other Membrane-Skeletal Proteins

Unfixed longitudinal cryosections of quadriceps muscle from control and *mdx* animals were labeled in double im-

muno fluorescence protocols for  $\beta$ -spectrin, with either 9050 or chicken anti- $\beta$ -spectrin antibodies, and with antibodies to other integral membrane or cytoskeletal proteins, including syntrophin,  $\beta$ -dystroglycan, vinculin, utro-

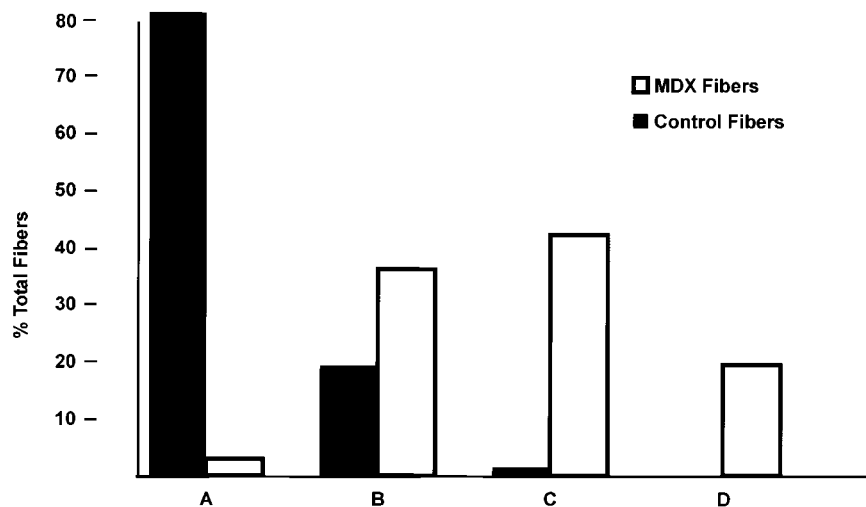


**Figure 3.** Quantitation of  $\beta$ -spectrin patterns in *mdx* fibers. Images of samples processed, as in Fig. 2, were evaluated double blind for the dominant patterns of  $\beta$ -spectrin distribution. Afterwards they were sorted into four categories: A, clear costameric distribution, including regular labeling over Z lines and M lines, and in longitudinal domains; B, labeling absent over M lines or in longitudinal domains; C, labeling absent both over M lines and in longitudinal domains; and D, labeling of polygonal arrays or other structures that do not demonstrate regular labeling over Z lines. 108 *mdx* fibers and 72 control fibers were examined. Closed bars: controls; open bars: *mdx*.

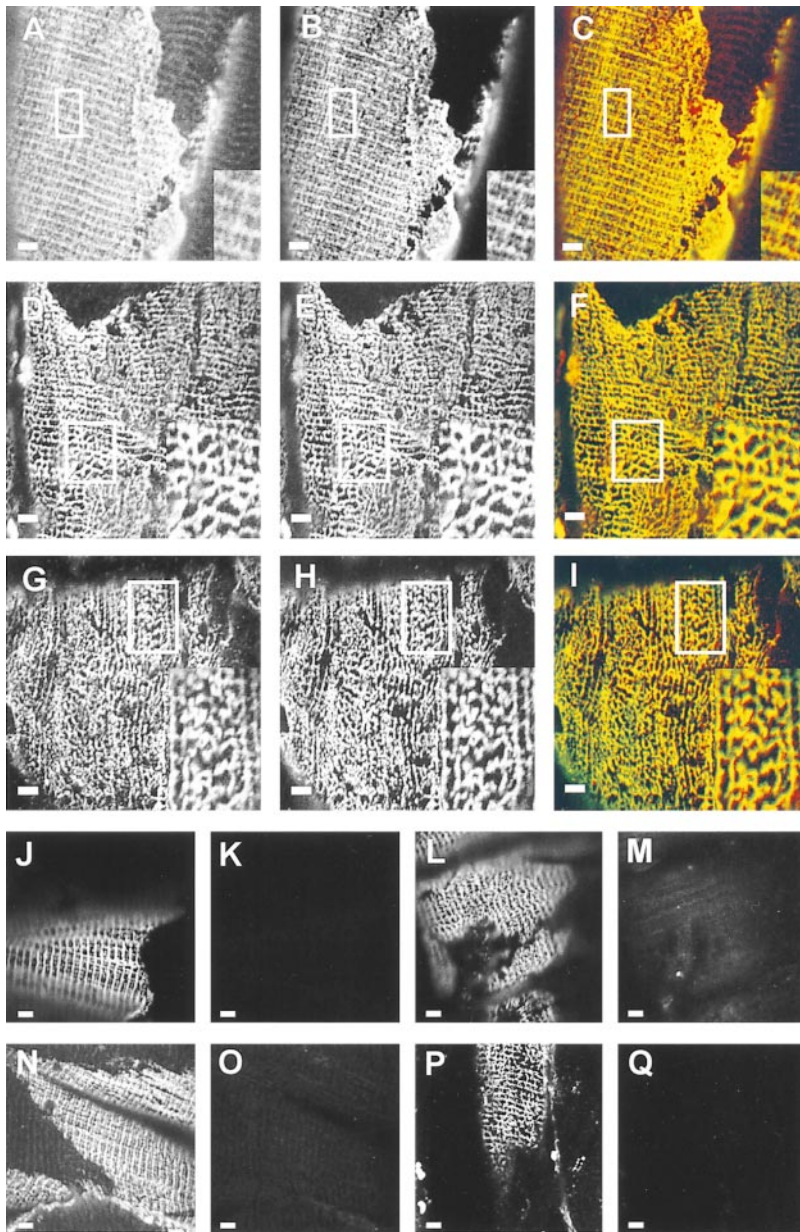


**Figure 4.** Altered distribution of the Na,K-ATPase at the sarcolemma of *mdx* muscle. Unfixed quadriceps muscles of wild-type (A–C, J–M) and *mdx* (D–I, N–Q) mice were snap frozen and sectioned on a cryostat. Experimental samples (A–I) were double-labeled with affinity-purified chicken antibodies to  $\beta$ -spectrin (B, E, and H) and polyclonal rabbit antibodies to the  $\alpha 1$  (A and D) or  $\alpha 2$  (G) subunits of the Na,K-ATPase. In color composite images, the  $\alpha 1$  or  $\alpha 2$  subunits are represented in red,  $\beta$ -spectrin in green, and sites containing both proteins in yellow. (A–C)  $\beta$ -Spectrin and the  $\alpha 1$  subunit of the Na,K-ATPase colocalize in costameres in control muscle fibers. Similar results were obtained with the  $\alpha 2$  subunit of the Na,K-ATPase (not shown). (D–I) The distribution of the  $\alpha 1$  (D) and  $\alpha 2$  (G) subunits of the Na,K-ATPase at the sarcolemma is altered, but these subunits still colocalize with the  $\beta$ -spectrin (yellow structures in F and I). (J–Q) Controls were double-labeled either with nonimmune chicken IgY (K and O) and rabbit antibodies to the  $\alpha 1$  subunit of the Na,K-ATPase (J and N), or with normal rabbit serum (L and P) and chicken anti- $\beta$ -spectrin (M and Q). No nonspecific labeling or bleedthrough of fluorescence was observed. Bars, 5  $\mu$ m.

phin, and the  $\alpha 1$  and  $\alpha 2$  subunits of the Na,K-ATPase. Structures labeled by primary antibodies were visualized with species-specific secondary antibodies coupled to either fluorescein or tetramethylrhodamine.

The  $\alpha 1$  and  $\alpha 2$  subunits of the Na,K-ATPase form a complex with ankyrin and  $\beta$ -spectrin at the sarcolemma of skeletal muscle fibers (Williams, M.W., and R.J. Bloch, manuscript in preparation). This results in the codistribution of the two subunits of the Na,K-ATPase with  $\beta$ -spectrin in costameres (for a typical control, see Fig. 4, A–C). Therefore, we expected both subunits to redistribute with  $\beta$ -spectrin at the sarcolemma of *mdx* muscle. This prediction was confirmed by double immunofluorescence experiments ( $\alpha 1$ : Fig. 4, D–F;  $\alpha 2$ : Fig. 4, G–I). We observed extensive overlap in the distributions of these proteins with  $\beta$ -spectrin (Fig. 4, C and F; in the color overlays, red repre-

sents the Na,K-ATPase, green represents  $\beta$ -spectrin and yellow represents regions containing both proteins). The absence of labeling at regions overlying M lines, the disruption of longitudinally oriented strands and structures overlying Z lines, and the presence of irregular polygonal structures were evident in the patterns of labeling of the  $\alpha 1$  and  $\alpha 2$  subunits of the Na,K-ATPase, as they were for  $\beta$ -spectrin.

$\beta$ -Dystroglycan is the transmembrane glycoprotein of the dystrophin-associated glycoprotein complex that binds dystrophin (39, 77). Syntrophin is a peripheral membrane protein that binds to dystrophin at sites COOH-terminal to those recognized by  $\beta$ -dystroglycan (2, 9). In control muscle fibers, both syntrophin and  $\beta$ -dystroglycan are enriched in costameres (Williams, M.W., and R.J. Bloch, manuscript in preparation), as previously reported for dys-



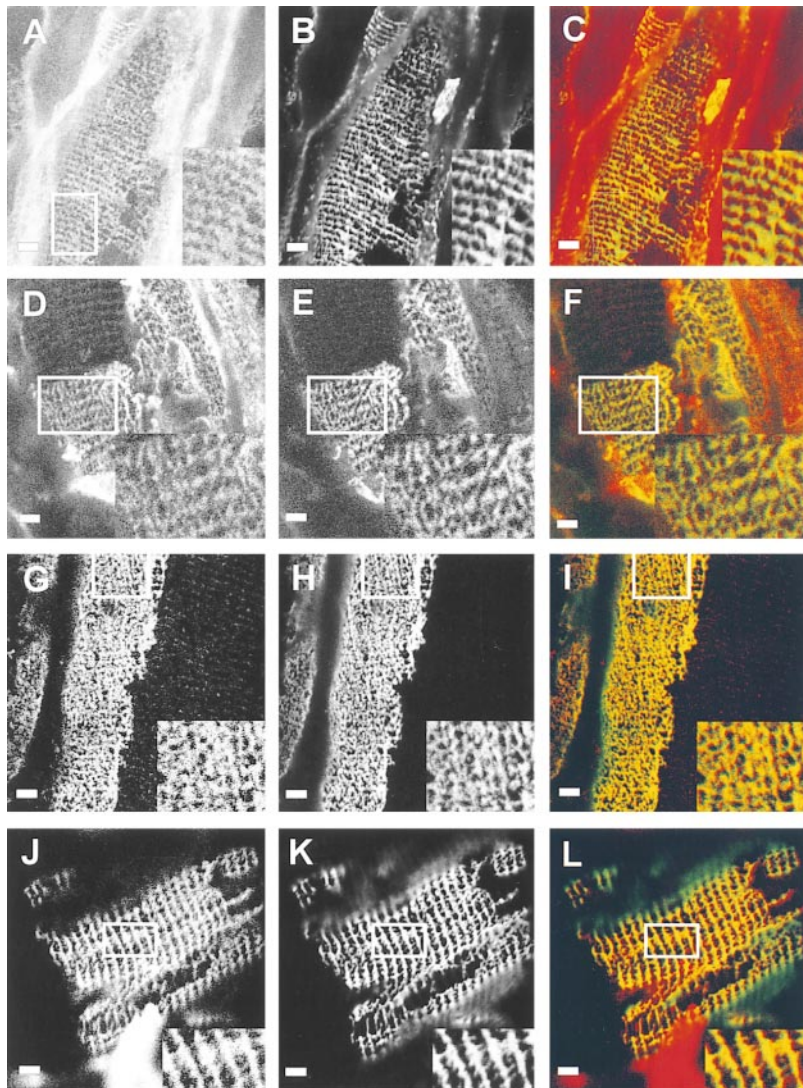


**Figure 5.** Altered distribution of syntrophin,  $\beta$ -dystroglycan, utrophin, and vinculin at the sarcolemma of *mdx* muscle. Perfusion-fixed quadriceps muscles from *mdx* mice were processed as in Fig. 2 and double-labeled with affinity-purified rabbit antibodies to  $\beta$ -spectrin (9050: B, E, H, and K) and mouse mAb to syntrophin (A),  $\beta$ -dystroglycan (D), vinculin (G), or utrophin (J). In composite pictures (C, F, I, and L),  $\beta$ -spectrin is shown in green, the other protein in red, and regions containing both proteins in yellow. The distribution of each of these proteins is altered in *mdx* muscle, but each continues to colocalize with  $\beta$ -spectrin (yellow structures in C, F, I, and L). Bars, 5  $\mu$ m.

trophin itself (see above). In *mdx* tissue, the amounts of  $\beta$ -dystroglycan and syntrophin decrease significantly, but low levels of both proteins can still be found at the sarcolemma (7, 56, 58). We used mAbs against  $\beta$ -dystroglycan or syntrophin together with 9050 anti- $\beta$ -spectrin to label longitudinal sections of *mdx* muscle. Both syntrophin and  $\beta$ -dystroglycan were enriched in costameric structures at the sarcolemma that lacked longitudinal strands and elements overlying M lines, as well as in regions of the sarcolemma that were more severely altered (Fig. 5, A and D). Comparison of  $\beta$ -spectrin with either  $\beta$ -dystroglycan or syntrophin demonstrated extensive colocalization (Fig. 5, C and F). Thus, the reduced amounts of syntrophin and  $\beta$ -dystroglycan at the sarcolemma of *mdx* muscle codistributed in the membrane skeleton together with  $\beta$ -spectrin.

Vinculin is a protein involved in the attachment of actin filaments to the membrane at focal adhesions (28) that is also found in costameres in skeletal muscle fibers (59, 69), where it codistributes with  $\beta$ -spectrin and dystrophin (62). We labeled *mdx* tissue with anti-vinculin mAbs and with 9050 anti- $\beta$ -spectrin. We found that the distribution of vinculin was also altered at the sarcolemma of the *mdx*

mouse. Like the proteins studied above, vinculin was much less regularly organized in *mdx* muscle than in control muscle, with gaps appearing because of the loss of longitudinal domains or domains overlying Z or M lines. Vinculin continued to colocalize with  $\beta$ -spectrin in these altered structures (Fig. 5, G–I). This result contradicts a recent report (51) stating that the organization of dystrophin, but not vinculin, was altered at the sarcolemma of muscle fibers from patients with Becker muscular dystrophy.

We also examined the distribution of utrophin expressed in *mdx* muscle (42, 46, 48, 86). Recent results with muscles that lack both dystrophin and utrophin (16, 30) support the idea that the expression of low levels of utrophin in *mdx* muscle may protect it from the severe damage seen in Duchenne patients (79). Labeling of *mdx* muscle by anti-utrophin antibodies was apparent over wide areas of the sarcolemma in the same kinds of altered arrays as described above. When we compared the distribution of utrophin to that of  $\beta$ -spectrin by double label immunofluorescence, utrophin codistributed with  $\beta$ -spectrin at the sarcolemma (Fig. 5, J–L).

Control experiments ensured that our observations



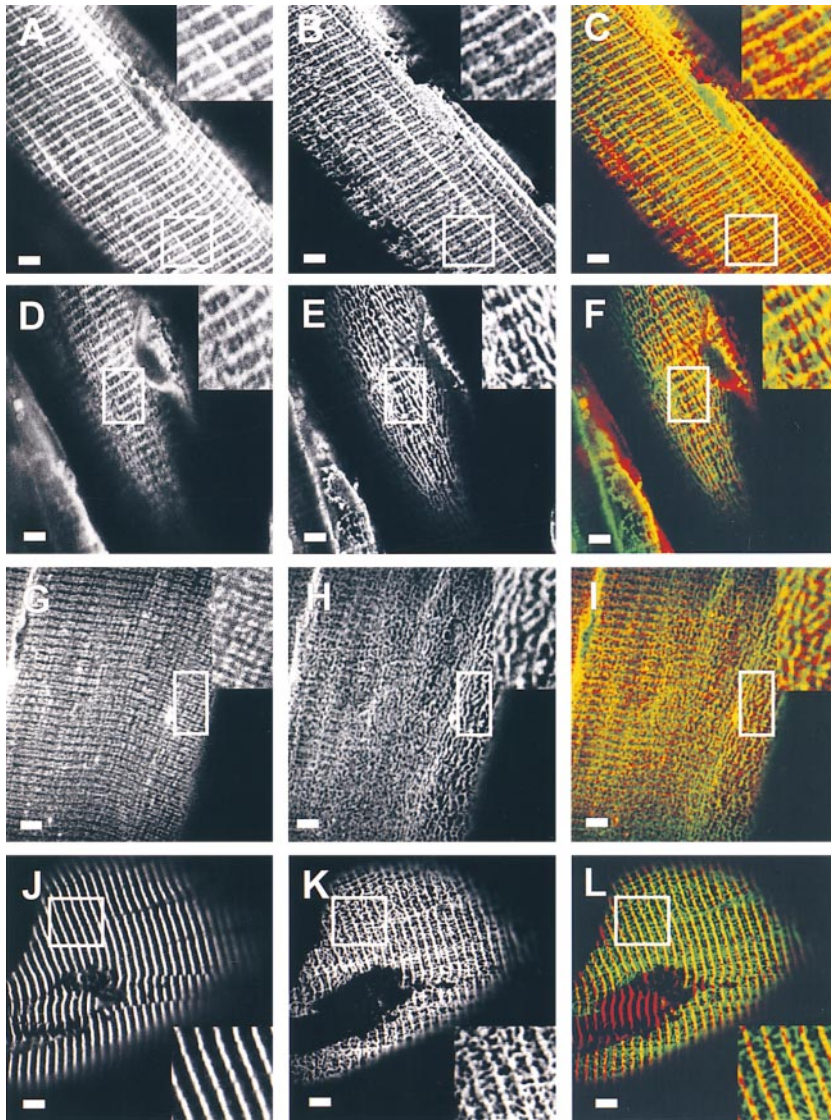


**Figure 6.** Unaltered distribution of intracellular proteins near the sarcolemma of *mdx* muscle. Samples of wild-type (A–C) and *mdx* (D–L) muscle were labeled with rabbit anti- $\beta$ -spectrin 9050 (B, E, H, and K) and mouse mAb to SERCA (A and D), DHPR (G), or  $\alpha$ -actinin (J). In composite images,  $\beta$ -spectrin is shown in green, the other proteins in red, and regions in the confocal plane that contain both proteins in yellow. (A–C) Near the sarcolemma of wild-type mouse skeletal muscle, SERCA is concentrated around Z lines, with additional elements around M lines and in longitudinally oriented domains. Labeling for SERCA in the sarcoplasmic reticulum around the M and Z lines appears to coincide with  $\beta$ -spectrin in the nearby sarcolemma (yellow structures in C), because of the  $\sim 1.2$ - $\mu\text{m}$  depth of the confocal plane sampled. Labeling in longitudinally oriented structures in the sarcoplasmic reticulum containing SERCA and similar structures at the sarcolemma containing  $\beta$ -spectrin are apparently not coordinated (red and green structures in C). (D–F) The concentration of SERCA in the sarcoplasmic reticulum at the levels of the Z and M lines, and in longitudinally oriented structures, does not change in the vicinity of the *mdx* sarcolemma, which shows an altered distribution of  $\beta$ -spectrin. (G–I) DHPR is normally concentrated in the t-tubules that surround each sarcomere at the A–I junction (see text). This also holds for t-tubules surrounding the A–I junctions of the myofibrils that lie near the *mdx* sarcolemma, despite the fact that the distribution of  $\beta$ -spectrin at the sarcolemma is changed. (J–L)  $\alpha$ -Actinin is normally concentrated in the Z disk (see text; Fig. 1); its distribution at Z disks of myofibrils in the vicinity of the *mdx* sarcolemma is not changed. Bars, 5  $\mu\text{m}$ .

were not due to cross-reaction of the species-specific secondary antibodies with inappropriate primary antibodies, or to bleedthrough of the fluorescent label from one channel into another (Fig. 1, G–L; Fig. 4, J–M). Antibodies to  $\beta$ -spectrin generated in chickens and used to label *mdx* and wild-type muscle, together with appropriate controls, gave the same results. Thus, it is unlikely that the coincident labeling for  $\beta$ -spectrin and the other membrane skeletal proteins at the sarcolemma of wild-type or *mdx* muscle fibers was artifactual. Therefore, our results suggest that several proteins that codistribute with  $\beta$ -spectrin in costameres at the sarcolemma of healthy muscle also codistribute with  $\beta$ -spectrin in the irregularly organized membrane skeleton of *mdx* myofibers.

### Intracellular Proteins

The changes we observed in the organization of the sarcolemma might simply reflect extensive changes in the cytoarchitecture of dystrophic myofibers (52). To assess the effects of the *mdx* phenotype on the organization of intra-

cellular structures lying near the dystrophic sarcolemma, we used antibodies to  $\alpha$ -actinin and to two integral membrane proteins of intracellular membranes, coupled with confocal laser scanning microscopy.  $\alpha$ -Actinin is the main component of the Z disc and may be involved in anchoring the connections between the costamere and the contractile apparatus near the Z line (for review see 71, 76). Double labeling with mouse mAbs to the sarcomeric form of  $\alpha$ -actinin and rabbit antibodies against  $\beta$ -spectrin (9050) showed  $\alpha$ -actinin distributed normally at Z lines (Fig. 6 J), even at sites near the sarcolemma that showed highly disrupted patterns of labeling for  $\beta$ -spectrin (Fig. 6 K). Thus  $\alpha$ -actinin does not become disorganized in *mdx* muscle, even at Z lines that are in close proximity to areas of the dystrophic sarcolemma with abnormal membrane skeletal arrays.

The Ca-ATPase of the sarcoplasmic reticulum (SERCA) and DHPR of the transverse tubules are also readily studied in double label immunofluorescence protocols. SERCA is normally distributed in tubular elements surrounding the Z line and M lines, as well as in elements aligned with the



longitudinal axis of the myofibers (Fig. 6, A–C). DHPR is easily visualized in mammalian muscle as a double line at the junctions of the A and I bands, where the transverse tubules surround each sarcomere, including those near the sarcolemma (38; for review see 25). The distributions of both these membrane proteins showed no evidence of an altered organization in *mdx* fibers, even when they were examined in the same confocal plane as the dystrophic sarcolemma, visualized with 9050 anti- $\beta$ -spectrin (SERCA: Fig. 6, D–F; DHPR, Fig. 6, G–I). These results suggest that the changes in the organization of muscle fibers in adult *mdx* mice are limited to the sarcolemma and closely associated proteins. This is consistent with ultrastructural studies that reveal little change in the sarcoplasm of adult *mdx* muscle (13, 80).

## Discussion

We used immunofluorescence labeling and confocal microscopy to examine the distribution of membrane skeletal proteins in healthy and dystrophic (*mdx*) mouse muscle. Our experiments were designed to test the hypothesis that the absence of dystrophin is accompanied by extensive changes in the organization of the sarcolemma. Our results strongly support this hypothesis by demonstrating widespread and potentially significant changes in the distribution of several peripheral and integral membrane proteins at the sarcolemma. Surprisingly, all the proteins we examined continued to codistribute at the altered sarcolemma despite the absence of dystrophin.

Earlier studies from this laboratory indicated the presence of  $\beta$ -spectrin in transverse structures overlying the Z lines and M lines, and in longitudinal strands (62). We noted that the  $\beta$ -spectrin pattern in muscle from *mdx* mice and from patients with Duchenne muscular dystrophy “always appeared less ordered than in controls” (62). Here we confirm and extend these earlier observations and show further that the extent of damage sustained by dystrophic myofibers can vary widely. This variability probably occurs because of differences in contractile activity and the load experienced in the period before sampling (41, 45, 68, 74), and previous cycles of degeneration and regeneration (14, 19, 53; for review see 22). Therefore, sampling a large number of myofibers may be necessary to reach any conclusions about the extent of spectrin-based membrane skeleton reorganization in dystrophic muscle.

Although much of our research has focused on  $\beta$ -spectrin, many other membrane-associated proteins codistribute with  $\beta$ -spectrin in irregular cytoskeletal arrays found at the dystrophic sarcolemma. These include all of the following: Na,K-ATPase, present in a complex with spectrin in skeletal muscle (Williams, M.W., and R.J. Bloch, manuscript in preparation); utrophin, the dystrophin homologue; two dystrophin-associated proteins, syntrophin and  $\beta$ -dystroglycan (for review see 9, 55); and vinculin, a protein normally found at focal adhesions and other plasmalemmal sites associated with organized bundles of actin microfilaments (for review see 11). The fact that all of these proteins are enriched in costameres of dystrophic and healthy skeletal muscle suggests that their organization is coordinated (however, see 51).

The identity of the protein (or proteins) responsible for

coordinating the distribution of proteins at the sarcolemma is still unclear. The most likely candidate is actin because it binds to dystrophin,  $\beta$ -spectrin, and vinculin, but the evidence that actin is enriched at costameres is minimal (12). Furthermore, mutations in dystrophin that eliminate its actin-binding activity produce mild phenotypes (9, 10, 84; however, see 3). If the extent of disorganization of the membrane-associated cytoskeleton is related to the severity of dystrophinopathy (see below), then the mild effects of these mutations would argue against a primary role for actin in coordinating the organization of dystrophin and its associated proteins with other membrane skeletal elements at the sarcolemma.

In contrast, loss of dystrophin's binding site for dystroglycan results in the severest dystrophinopathies (9, 65). This suggests that dystroglycan or other ligands (e.g.,  $\gamma$ -sarcoglycan; ref. 31) interacting with the COOH-terminal region of dystrophin may be the primary organizers. For example, syntrophin binds to the voltage-gated sodium channel (27) that also associates with spectrin through ankyrin (72), suggesting that it may link the spectrin-based membrane skeleton to dystrophin in healthy muscle. However, as deletion of the syntrophin binding site in the COOH-terminal region of dystrophin (2) is not associated with myopathy in mice (65), syntrophin–dystrophin interactions are probably not required to maintain the integrity of the sarcolemma.

Utrophin, expressed in *mdx* muscle (42, 46, 48, 86), may partially substitute for dystrophin at the sarcolemma (79). Although it concentrates at the sarcolemma and binds to many of the same ligands as dystrophin, utrophin is unlikely to organize sarcolemmal spectrin and vinculin. Utrophin is present in *mdx* muscle at levels significantly lower than the levels of dystrophin in wild-type muscle, but levels of spectrin and vinculin are not appreciably reduced in *mdx* muscle (our unpublished observations). Thus, if utrophin does help to link the dystrophin-associated cytoskeleton to spectrin and vinculin at the sarcolemma, the stoichiometry of this linkage must differ significantly from that present in normal muscle. Furthermore, although utrophin, dystrophin, and spectrin have been shown to codistribute in a membrane skeletal network in cultures of rat myotubes, this network does not contain vinculin (18, 64; Bloch et al., manuscript in preparation). These results suggest that utrophin is unlikely to coordinate the organization of the various membrane skeletal proteins in *mdx* muscle fibers.

Although the proteins that organize the membrane skeleton in dystrophic muscle must still be identified, dystrophin clearly plays an important role in maintaining the organization of the membrane skeleton in normal muscle. In dystrophinopathies, several of the structural domains at the sarcolemma of wild-type muscle tend to disappear. However, the nature of the relationship between this reorganization of the membrane skeleton and the absence of dystrophin in *mdx* muscle fibers is still not clear.

The reorganization of the membrane skeleton in *mdx* myofibers may be an indirect result of the absence of dystrophin, perhaps related to changes in  $\text{Ca}^{2+}$  homeostasis (21, 33, 36, 44, 66, 78).  $\text{Ca}^{2+}$ -dependent proteases, such as calpain and caspases, activated by  $\text{Ca}^{2+}$  entering the myofiber through the dystrophic sarcolemma, are capable of

cleaving spectrins (34, 61, 67, 81) and other structural proteins (29). The proteolysis of spectrin, coupled with the absence of dystrophin, might disrupt the membrane-associated cytoskeleton sufficiently to destabilize sarcolemmal organization. This model predicts an increase in *mdx* muscle of proteolytic fragments of spectrin, perhaps associated with the altered costameric structures described here.

Alternatively, the changes in sarcolemmal organization may not be directly linked to the absence of dystrophin at all. For example, they may be related to the stage of muscle regeneration reached by each dystrophic myofiber at the time of sampling. The polygonal arrays seen in a small percentage of *mdx* fibers also appear in myofibers developing in vivo (our unpublished results). However, myofibers in the *mdx* mouse tend to undergo only a single cycle of degeneration and regeneration occurring 3–5 wk after birth. Afterwards, only a small number of muscle fibers degenerate at any given time (13, 14, 53). As our current studies were limited to 6-mo-old animals, it is unlikely that this alone can account for our observation that the membrane skeleton is significantly altered in >90% of *mdx* muscle fibers (Fig. 3).

Our results may also be interpreted in terms of models that invoke a direct role for dystrophin in organizing the membrane skeleton in healthy muscle fibers. For example, dystrophin in healthy muscle may stabilize the costameric sites at which membrane skeletal proteins accumulate. Therefore, the absence of dystrophin in *mdx* muscles may render their membrane skeleton more susceptible to distortion and disruption by the forces exerted on the sarcolemma during muscle contraction and relaxation. This suggests that the membrane domains most easily disrupted at the sarcolemma are the longitudinal strands and the structures lying over M lines. These are more readily lost in *mdx* muscle, whereas sarcolemmal structures located over Z lines are more stable. Our previous studies of fast twitch rat muscle fibers have shown that the domains over Z lines contain  $\beta$ -spectrin complexed with  $\alpha$ -fodrin, whereas the longitudinal strands and domains over M lines contain  $\beta$ -spectrin with little  $\alpha$ -fodrin or any other  $\alpha$  subunit of the spectrin superfamily that we have been able to identify (63). Such differences in the structure of membrane-bound spectrin may account for the greater instability of longitudinal and M line domains in *mdx* muscle.

Structural differences may also explain why normal contractions lead to damage and degeneration of dystrophic muscle fibers. The altered organization of costameres suggests that the connections between the sarcolemma and the sarcomeres of superficial myofibrils are not as periodic in *mdx* muscle as they are in controls. In healthy myofibers, these connections mediate the transmission of force from the contractile apparatus to the sarcolemma and the extracellular matrix, while keeping the sarcolemma in close register with the underlying myoplasm during the contractile cycle (75). The reduced number and the abnormal arrangement of such connections are likely to render the dystrophic sarcolemma more fragile than controls.

Disruption of the membrane skeleton of *mdx* also generates regions of the sarcolemma that are devoid of costameres. These regions can cover relatively large areas (>50  $\mu\text{m}^2$ ; e.g., Fig. 2 H, regions of the sarcolemma between neighboring Z lines). In normal fast twitch muscle

fibers of the rat, where longitudinal strands and structures overlying M lines are normally present, the regions between costameres usually do not exceed 2  $\mu\text{m}^2$  in area, and even these small regions are likely to be stabilized by low levels of dystrophin (Williams, M.W., and R.J. Bloch, manuscript in preparation). This protein is, of course, absent in *mdx* muscle. The gaps in the membrane skeleton of dystrophic myofibers are considerably smaller than the "delta lesions" documented in samples of Duchenne muscle (52), and unlike delta lesions they appear to be limited to structures at or immediately adjacent to the sarcolemma. Nevertheless, areas lacking a membrane skeleton may be especially susceptible to damage; indeed, they may even be the sites at which lesions are initiated. The reorganization of the sarcolemma and the appearance of gaps in the membrane skeleton may therefore lead directly to the damage sustained by dystrophic muscle fibers. It follows that measuring the reduction in the number and size of these gaps may provide a sensitive and quantitative way to test therapies now being developed to treat Duchenne muscular dystrophy.

This paper is dedicated to Guido Guidotti on his 65th birthday.

We are grateful to Ms. W.G. Resneck and A. O'Neill for their assistance at different stages of this research, to Dr. S.C. Froehner (University of North Carolina, Chapel Hill, NC) for his gift of antibodies to syntrophin and to DHP, to Drs. N.C. Porter, J. Ursitti, D.W. Pumplin, W.R. Randall, M.P. Blaustein, and M.F. Schneider (University of Maryland School of Medicine, Baltimore, MD) for useful discussions, and to the reviewers for their constructive criticism.

Our research has been supported by grants to R.J. Bloch from the National Institutes of Health (NS 17282) and from the Muscular Dystrophy Association.

Received for publication 23 November 1998 and in revised form 9 February 1999.

## References

1. Ahn, A.H., and L.M. Kunkel. 1993. The structural and functional diversity of dystrophin. *Nat. Genet.* 3:283–291.
2. Ahn, A.H., and L.M. Kunkel. 1995. Syntrophin binds to an alternatively spliced exon of dystrophin. *J. Cell Biol.* 128:363–371.
3. Amann, K.J., B.A. Renley, and J.M. Ervasti. 1998. A cluster of basic repeats in the dystrophin rod domain binds F-actin through an electrostatic interaction. *J. Biol. Chem.* 273:28419–28423.
4. Bewick, G.S., L.V. Nicholson, C. Young, E. O'Donnell, and C.R. Slater. 1992. Different distributions of dystrophin and related proteins at nerve-muscle junctions. *NeuroReport.* 3:857–860.
5. Bewick, G.S., L.V. Nicholson, C. Young, and C.R. Slater. 1993. Relationship of a dystrophin-associated glycoprotein to junctional acetylcholine receptor clusters in rat skeletal muscle. *Neuromuscul. Disord.* 3:503–506.
6. Blufield, G., W.G. Siller, A.L. Wight, and K.J. Moore. 1984. X chromosome-linked muscular dystrophy (*mdx*) in the mouse. *Proc. Natl. Acad. Sci. USA.* 81:1189–1192.
7. Butler, M.H., K. Douville, A.A. Murnane, N.R. Kramarcy, J.B. Cohen, R. Sealock, and S.C. Froehner. 1992. Association of the M<sub>1</sub>, 58,000 postsynaptic protein of electric tissue with *Torpedo* dystrophin and the M<sub>1</sub>, 87,000 postsynaptic protein. *J. Biol. Chem.* 267:6213–6218.
8. Campbell, K.P., and S.D. Kahl. 1989. Association of dystrophin and an integral membrane glycoprotein. *Nature.* 338:259–262.
9. Chamberlain, J.S., K. Corrado, J.A. Rafael, G.A. Cox, M. Hauser, and C. Lumeng. 1997. Interactions between dystrophin and the sarcolemma membrane. In *Cytoskeletal Regulation of Membrane Function*. S.C. Froehner and V. Bennett, editors. The Rockefeller University Press, New York, 19–29.
10. Corrado, K., J.A. Rafael, P.L. Mills, N.M. Cole, J.A. Faulkner, K. Wang, and J.S. Chamberlain. 1996. Transgenic *mdx* mice expressing dystrophin with a deletion in the actin-binding domain display a "mild Becker" phenotype. *J. Cell Biol.* 134:873–884.
11. Craig, S.W., and R.P. Johnson. 1996. Assembly of focal adhesions: progress, paradigms, and portents. *Curr. Opin. Cell Biol.* 8:74–85.
12. Craig, S.W., and J.V. Pardo. 1983. Gamma actin, spectrin, and intermediate filament proteins colocalize with vinculin at costameres, myofibril-to-sar-

- colemma attachment sites. *Cell Motil.* 3:449-462.
13. Cullen, M.J., and E. Jaros. 1988. Ultrastructure of the skeletal muscle in the X chromosome-linked dystrophic (*mdx*) mouse. Comparison with Duchenne muscular dystrophy. *Acta Neuropathol.* 77:69-81.
  14. Dangain, J., and G. Vrbova. 1984. Muscle development in *mdx* mutant mice. *Muscle Nerve.* 7:700-704.
  15. Davison, M.D., and D.R. Critchley. 1988. Alpha-actinins and the DMD protein contain spectrin-like repeats. *Cell.* 52:159-160.
  16. Deconinck, A.E., J.A. Rafael, J.A. Skinner, S.C. Brown, A.C. Potter, L. Metzinger, D.J. Watt, J.G. Dickson, J.M. Tinsley, and K.E. Davies. 1997. Utrophin-dystrophin-deficient mice as a model for Duchenne muscular dystrophy. *Cell.* 90:717-727.
  17. Dhermy, D. 1991. The spectrin super-family. *Biol. Cell.* 71:249-254.
  18. Dmytrenko, G.M., D.W. Pumplin, and R.J. Bloch. 1993. Dystrophin in a membrane skeletal network: localization and comparison to other proteins. *J. Neurosci.* 13:547-558.
  19. Dupont-Versteegden, E.E., and R.J. McCarter. 1992. Differential expression of muscular dystrophy in diaphragm versus hindlimb muscles of *mdx* mice. *Muscle Nerve.* 15:1105-1110.
  20. Ehmer, S., R. Herrmann, R. Bittner, and T. Voit. 1997. Spatial distribution of  $\beta$ -spectrin in normal and dystrophic human skeletal muscle. *Acta Neuropathol.* 94:240-246.
  21. Emery, A.E.H. 1990. Dystrophin function. *Lancet (N. Am. Ed.).* 335:1289-1289.
  22. Emery, A.E.H. 1993. Duchenne Muscular Dystrophy. Oxford University Press, Oxford, U.K. 392 pp.
  23. Engel, A.G. 1994. Dystrophinopathies. In *Myology*. A.G. Engel and C. Franzini-Armstrong, editors. McGraw-Hill, New York. 1130-1187.
  24. England, S.B., L.V. Nicholson, M.A. Johnson, S.M. Forrest, D.R. Love, E.E. Zubrzycka-Gaarn, D.E. Bulman, J.B. Harris, and K.E. Davies. 1990. Very mild muscular dystrophy associated with the deletion of 46% of dystrophin. *Nature.* 343:180-182.
  25. Franzini-Armstrong, C. 1994. The sarcoplasmic reticulum and the transverse tubules. In *Myology*. A.G. Engel and C. Franzini-Armstrong, editors. McGraw-Hill, New York. 176-199.
  26. Gee, S.H., R.W. Blacher, P.J. Douville, P.R. Provost, P.D. Yurchenco, and S. Carbonetto. 1993. Laminin-binding protein 120 from brain is closely related to the dystrophin-associated glycoprotein, dystroglycan, and binds with high affinity to the major heparin binding domain of laminin. *J. Biol. Chem.* 268:14972-14980.
  27. Gee, S.H., R. Madhavan, S.R. Levinson, J.H. Caldwell, R. Sealock, and S.C. Froehner. 1998. Interaction of muscle and brain sodium channels with multiple members of the syntrophin family of dystrophin-associated proteins. *J. Neurosci.* 18:128-137.
  28. Geiger, B. 1979. A 130K protein from chicken gizzard: its localization at the termini of microfilament bundles in cultured chicken cells. *Cell.* 18:193-205.
  29. Goll, D.E., V.F. Thompson, R.G. Taylor, and J.A. Christiansen. 1992. Role of the calpain system in muscle growth. *Biochimie (Paris).* 74:225-237.
  30. Grady, R.M., H. Teng, M.C. Nichol, J.C. Cunningham, R.S. Wilkinson, and J.R. Sanes. 1997. Skeletal and cardiac myopathies in mice lacking utrophin and dystrophin: a model for Duchenne muscular dystrophy. *Cell.* 90:729-738.
  31. Hack, A.A., C.T. Ly, F. Jiang, C.J. Clendenin, K.S. Sigrist, R.L. Wollmann, and E.M. McNally. 1998. Gamma-sarcoglycan deficiency leads to muscle membrane defects and apoptosis independent of dystrophin. *J. Cell Biol.* 142:1279-1287.
  32. Herrmann, R., L.V. Anderson, and T. Voit. 1996. Costameric distribution of beta-dystroglycan (43kDa dystrophin-associated glycoprotein) in normal and dystrophin-deficient human skeletal muscle. *Biochem. Soc. Trans.* 24:501-506.
  33. Hopf, F.W., P.R. Turner, W.F. Denetclaw, P. Reddy, and R.A. Steinhart. 1996. A critical evaluation of resting intracellular free calcium regulation in dystrophic *mdx* muscle. *Am. J. Physiol.* 271:C1325-C1339.
  34. Hu, R.-J., and V. Bennett. 1991. In vitro proteolysis of brain spectrin by calpain I inhibits association of spectrin with ankyrin-independent membrane binding site(s). *J. Biol. Chem.* 266:18200-18205.
  35. Ibraghimov-Beskrovnaia, O., J.M. Ervasti, C.J. Leveille, C.A. Slaughter, S.W. Sernett, and K.P. Campbell. 1992. Primary structure of dystrophin-associated glycoproteins linking dystrophin to the extracellular matrix. *Nature.* 355:696-702.
  36. Imbert, N., C. Cognard, G. Dupont, C. Guillou, and G. Raymond. 1998. Abnormal calcium homeostasis in Duchenne muscular dystrophy myotubes contracting in vitro. *Cell Calcium.* 18:177-186.
  37. Johnson, G.D., R.S. Davidson, K.C. McNamee, G. Russell, D. Goodwin, and E.J. Holborow. 1982. Fading of immunofluorescence during microscopy: a study of the phenomenon and its remedy. *J. Immunol. Methods.* 55:231-242.
  38. Jorgensen, A.O., A.C.Y. Shen, W. Arnold, A.T. Leung, and K.P. Campbell. 1989. Subcellular distribution of the 1,4-dihydropyridine receptor in rabbit skeletal muscle in situ: an immunofluorescence and immunocolloidal gold-labeling study. *J. Cell Biol.* 109:135-147.
  39. Jung, D., B. Yang, J. Meyer, J.S. Chamberlain, and K.P. Campbell. 1995. Identification and characterization of the dystrophin anchoring site on  $\beta$ -dystroglycan. *J. Biol. Chem.* 270:27305-27310.
  40. Kahana, E., and W.B. Gratzner. 1995. Minimum folding unit of dystrophin rod domain. *Biochemistry.* 34:8110-8114.
  41. Karpati, G., S. Carpenter, and S. Prescott. 1988. Small-caliber skeletal muscle fibers do not suffer necrosis in *mdx* mouse dystrophy. *Muscle Nerve.* 11:795-803.
  42. Khurana, T.S., S.C. Watkins, P. Chafey, J. Chelly, F.M. Tome, M. Fardeau, J.C. Kaplan, and L.M. Kunkel. 1991. Immunolocalization and developmental expression of dystrophin related protein in skeletal muscle. *Neuromuscul. Disord.* 1:185-194.
  43. Koenig, M., A.P. Monaco, and L.M. Kunkel. 1988. The complete sequence of dystrophin predicts a rod-shaped cytoskeletal protein. *Cell.* 53:219-226.
  44. Leijendekker, W.J., A.C. Passaquin, L. Metzinger, and U.T. Ruegg. 1996. Regulation of cytosolic calcium in skeletal muscle cells of the *mdx* mouse under conditions of stress. *Br. J. Pharmacol.* 118:611-616.
  45. Louboutin, J.P., V. Fichter-Gagnepain, E. Thaon, and M. Fardeau. 1993. Morphometric analysis of *mdx* diaphragm muscle fibres. Comparison with hindlimb muscles. *Neuromuscul. Disord.* 3:463-469.
  46. Man, N.T., J.M. Ellis, D.R. Love, K.E. Davies, K.C. Gatter, G. Dickson, and G.E. Morris. 1991. Localization of the DMDL gene-encoded dystrophin-related protein using a panel of nineteen mAbs: presence at neuromuscular junctions, in the sarcolemma of dystrophic skeletal muscle, in vascular and other smooth muscles, and in proliferating brain cell lines. *J. Cell Biol.* 115:1695-1700.
  47. Masuda, T., N. Fujimaki, E. Ozawa, and H. Ishikawa. 1992. Confocal laser microscopy of dystrophin localization in guinea pig skeletal muscle fibers. *J. Cell Biol.* 119:543-548.
  48. Matsumura, K., J.M. Ervasti, K. Ohlendieck, S.D. Kahl, and K.P. Campbell. 1992. Association of dystrophin-related protein with dystrophin-associated proteins in *mdx* mouse muscle. *Nature.* 360:588-591.
  49. Minetti, C., F. Beltrame, G. Marcenaro, and E. Bonilla. 1992. Dystrophin at the plasma membrane of human muscle fibers shows a costameric localization. *Neuromuscul. Disord.* 2:99-109.
  50. Minetti, C., K. Tanji, P.G. Rippa, G. Morreale, G. Cordone, and E. Bonilla. 1994. Abnormalities in the expression of  $\beta$ -spectrin in Duchenne muscular dystrophy. *Neurology.* 44:1149-1153.
  51. Minetti, C., G. Cordone, F. Beltrame, M. Bado, and E. Bonilla. 1998. Disorganization of dystrophin costameric lattice in Becker muscular dystrophy. *Muscle Nerve.* 21:211-216.
  52. Mokri, B., and A.G. Engel. 1975. Duchenne dystrophy: electron microscopic findings pointing to a basic or early abnormality in the plasma membrane of the muscle fiber. *Neurology.* 25:1111-1120.
  53. Muntoni, F., A. Mateddu, F. Marchei, A. Clerik, and G. Serra. 1993. Muscular weakness in the *mdx* mouse. *J. Neurol. Sci.* 120:71-77.
  54. Nicholson, L.V., K. Davison, G. Falkous, C. Harwood, E. O'Donnell, C.R. Slater, and J.B. Harris. 1989. Dystrophin in skeletal muscle. I. Western blot analysis using a monoclonal antibody. *J. Neurol. Sci.* 94:125-136.
  55. Ohlendieck, K. 1996. Towards an understanding of the dystrophin-glycoprotein complex: linkage between the extracellular matrix and the membrane cytoskeleton in muscle fibers. *Eur. J. Cell Biol.* 69:1-10.
  56. Ohlendieck, K., and K.P. Campbell. 1991. Dystrophin-associated proteins are greatly reduced in skeletal muscle from *mdx* mice. *J. Cell Biol.* 115:1685-1694.
  57. Ohlendieck, J., J.M. Ervasti, J.B. Snook, and K.P. Campbell. 1991. Dystrophin-glycoprotein complex is highly enriched in isolated skeletal muscle sarcolemma. *J. Cell Biol.* 112:135-148.
  58. Ohlendieck, K., K. Matsumura, V.V. Ionasescu, J.A. Towbin, E.P. Bosch, S.L. Weinstein, S.W. Sernett, and K.P. Campbell. 1993. Duchenne muscular dystrophy: deficiency of dystrophin-associated proteins in the sarcolemma. *Neurology.* 43:795-800.
  59. Pardo, J.V., J.D. Siliciano, and S.W. Craig. 1983. A vinculin-containing cortical lattice in skeletal muscle: transverse lattice elements ("costameres") mark sites of attachment between myofibrils and sarcolemma. *Proc. Natl. Acad. Sci. USA.* 80:1008-1012.
  60. Pierobon-Bormioli, S. 1981. Transverse sarcomere filamentous systems: "Z- and M-cables." *J. Musc. Res. Cell Motil.* 2:401-413.
  61. Pike, B.R., X. Zhao, J.K. Newcomb, R.M. Posmantur, K.K. Wang, and R.L. Hayes. 1998. Regional calpain and caspase-3 proteolysis of alpha-spectrin after traumatic brain injury. *NeuroReport.* 9:2437-2442.
  62. Porter, G.A., G.M. Dmytrenko, J.C. Winkelman, and R.J. Bloch. 1992. Dystrophin colocalizes with  $\beta$ -spectrin in distinct subsarcolemmal domains in mammalian skeletal muscle. *J. Cell Biol.* 117:997-1005.
  63. Porter, G.A., M.G. Scher, W.G. Resneck, V. Fowler, and R.J. Bloch. 1997. Two populations of  $\beta$ -spectrin in mammalian skeletal muscle. *Cell Motil. Cytoskeleton.* 37:7-19.
  64. Pumplin, D.W. 1995. The membrane skeleton of acetylcholine receptor domains in rat myotubes contains antiparallel homodimers of  $\beta$ -spectrin in filaments quantitatively resembling those of erythrocytes. *J. Cell Sci.* 108:3145-3154.
  65. Rafael, J.A., G.A. Cox, K. Corrado, D. Jung, K.P. Campbell, and J.S. Chamberlain. 1996. Forced expression of dystrophin deletion constructs reveals structure-function correlations. *J. Cell Biol.* 134:93-102.
  66. Reeve, J.L., A. McArdle, and M.J. Jackson. 1997. Age-related changes in muscle calcium content in dystrophin-deficient *mdx* mice. *Muscle Nerve.* 20:357-360.



67. Saatman, K.E., D. Bozyczko-Coyne, V. Marcy, R. Siman, and T.K. McIntosh. 1996. Prolonged calpain-mediated spectrin breakdown occurs regionally following experimental brain injury in the rat. *J. Neuropathol. Exp. Neurol.* 55:850-860.
68. Sacco, P., D.A. Jones, J.R.T. Dick, and G. Vrbova. 1992. Contractile properties and susceptibility to exercise-induced damage of normal and *mdx* mouse tibialis anterior muscle. *Clin. Sci.* 82:227-236.
69. Shear, C.R., and R.J. Bloch. 1985. Vinculin in subsarcolemmal densities in chicken skeletal muscle: localization and relationship to intracellular and extracellular structures. *J. Cell Biol.* 101:240-256.
70. Smalheiser, N.R. 1993. Cranin interacts specifically with the sulfatide-binding domain of laminin. *J. Neurosci. Res.* 36:528-538.
71. Small, J.V., D.O. Furst, and L.-E. Thornell. 1992. The cytoskeletal lattice of muscle cells. *Eur. J. Biochem.* 208:559-572.
72. Srinivasan, Y., L. Elmer, J. Davis, V. Bennett, and K. Angelides. 1988. Ankyrin and spectrin associate with voltage-dependent sodium channels in brain. *Nature.* 333:177-180.
73. Straub, V., R.E. Bittner, J.J. Leger, and T. Voit. 1992. Direct visualization of the dystrophin network on skeletal muscle fiber membrane. *J. Cell Biol.* 119:1183-1191.
74. Straub, V., J.A. Rafael, J.S. Chamberlain, and K.P. Campbell. 1997. Animal models for muscular dystrophy show different patterns of sarcolemmal disruption. *J. Cell Biol.* 139:375-385.
75. Street, S.F. 1983. Lateral transmission of tension in frog myofibers: a myofibrillar network and transverse cytoskeletal connections are possible transmitters. *J. Cell. Physiol.* 114:346-364.
76. Stromer, M.H. 1995. Immunocytochemistry of the muscle cell cytoskeleton. *Microsc. Res. Tech.* 31:95-105.
77. Suzuki, A., M. Yoshida, H. Yamamoto, and E. Ozawa. 1992. Glycoprotein-binding site of dystrophin is confined to the cysteine-rich domain and the first half of the carboxy-terminal domain. *FEBS Lett.* 308:154-160.
78. Tay, J.S., P.S. Lai, P.S. Low, W.L. Lee, and G.C. Gan. 1992. Pathogenesis of Duchenne muscular dystrophy: the calcium hypothesis revisited. *J. Paediatr. Child Health.* 28:291-293.
79. Tinsley, J.M., and K.E. Davies. 1993. Utrophin: a potential replacement for dystrophin? *Neuromusc. Disord.* 3:537-539.
80. Torres, L.F., and L.W. DuChen. 1987. The mutant *mdx*: inherited myopathy in the mouse. Morphological studies of nerves, muscles and end-plates. *Brain.* 110:269-299.
81. Wang, K.K., R.M. Posmantur, R. Nath, K. McGinnis, M. Whitton, R.V. Talanian, S.B. Glantz, and J.S. Morrow. 1998. Simultaneous degradation of alphaII- and betaII-spectrin by caspase 3 (CPP32) in apoptotic cells. *J. Biol. Chem.* 273:22490-22497.
82. Webster, C., L. Silberstein, A.P. Hays, and H.M. Blau. 1988. Fast muscle fibers are preferentially affected in Duchenne's muscular dystrophy. *Cell.* 52:503-513.
83. Wilson, T. 1986. Confocal light microscopy. *Ann. NY Acad. Sci.* 483:416-427.
84. Winnard, A.V., J.R. Mendell, T.W. Prior, J. Florence, and A.H. Burghes. 1995. Frameshift deletions of exons 3-7 and revertant fibers in Duchenne muscular dystrophy: mechanisms of dystrophin production. *Am. J. Hum. Genet.* 56:158-165.
85. Yoshida, M., and E. Ozawa. 1990. Glycoprotein complex anchoring dystrophin to sarcolemma. *J. Biochem.* 108:748-752.
86. Zhao, J.-E., K. Yoshioka, T. Miike, and M. Miyatake. 1993. Developmental studies of dystrophin-positive fibers in *mdx*, and DRP localization. *J. Neurol. Sci.* 114:104-108.
87. Zhou, D., J.A. Ursitti, and R.J. Bloch. 1998. Developmental expression of spectrins in rat skeletal muscle. *Mol. Biol. Cell.* 9:47-61.